

Impact of Direct-Drive WEC Systems on the Design of a Small PM Wind Generator

M. A. Khan, *Student Member, IEEE*, P. Pillay, *Senior Member, IEEE*, and M. Malengret

Abstract— Direct-drive wind energy conversion systems (WECS) are required to operate at low speeds determined by that of the turbine. This paper addresses the problem of adapting a small, standard, readily available PM synchronous machine for direct coupling to a small wind turbine. In particular, it investigates several minor changes to the machine design, which will ensure that rated power can be delivered to its load, whilst operating at the reduced speeds required by a direct-drive WECS.

Index Terms—Permanent magnet generators, synchronous generators, wind energy

I. NOMENCLATURE

E_f	- Excitation voltage
V_a	- Armature / terminal voltage per-phase
I_a	- Armature / load current
R_a	- Armature winding resistance per-phase
X_s	- Synchronous reactance
δ	- Load angle
ϕ	- Generator load power factor angle
Z_L	- Load impedance per-phase
R_L	- Load resistance per-phase
X_L	- Load reactance per-phase
P_L	- Total real power to the load on the generator

II. INTRODUCTION

Direct-drive wind energy conversion systems (WECS) are receiving increasing attention due to their inherent efficiency. By eliminating the need for a gearbox between the wind turbine and generator, these systems are less expensive and also require less maintenance. These systems are however required to operate at reduced speeds, determined by that of the turbine shaft.

This paper addresses the problem of adapting a small, standard, readily available PM synchronous machine for direct coupling to a small wind turbine. In particular, it investigates several minor changes to the machine design, which will ensure that rated power can be delivered to its load, whilst operating at the reduced speeds required by a direct-drive WECS.

This is accomplished by assembling an analytical model of a small PM synchronous machine. The analytical model is then used in conjunction with the terminal voltage characteristic and operating power capability of a small PM wind generator, to evaluate the effects of the design changes

on the performance of the machine.

III. ANALYTICAL MODEL OF A PM SYNCHRONOUS MACHINE

The analytical model of a small PM synchronous machine presented in this section is obtained by detailed consideration of its design equations. The model relates the electrical equivalent circuit parameters and performance of the machine to its mechanical design specifications. It neglects saturation effects of the magnetic circuit.

The machine under investigation in this paper is a 3.5kW, 8 pole, three-phase PM synchronous machine. It has radially magnetised NdFeB PMs mounted on the surface of a solid mild-steel rotor core. The resulting airgap flux density produced by the PMs is approximately rectangular in shape. The machine stator has a full-pitched, distributed, double-layer three-phase winding accommodated in semi-closed oval slots. The nominal design specifications of the machine are summarised in Table V of the Appendix.

A. Excitation Voltage

The rms value of the fundamental component of the excitation voltage induced in a phase winding of the machine can be expressed as [1]:

$$E_f = \frac{2\pi}{\sqrt{2}} f N_{ph} K_{w1} \phi_p \quad (1)$$

where K_{w1} is the fundamental harmonic winding factor and ϕ_p is the flux per pole due to the fundamental space harmonic component of the excitation flux density distribution.

The flux per pole can be expressed as [1]:

$$\phi_p = B_{1max} lD/p \quad (2)$$

where B_{1max} is the peak value of the fundamental space harmonic component of the excitation flux density distribution.

Furthermore, B_{1max} can be related to the plateau value B_g of the rectangular airgap flux density distribution produced by the PMs, as follows [2]:

$$B_{1max} = k_f B_g \quad (3)$$

where k_f is the form factor of the excitation field.

In the case of a single smooth PM per pole, k_f can be expressed as [2]:

$$k_f = \frac{4}{\pi} \sin\left(\frac{\alpha\pi}{2}\right) \quad (4)$$

The plateau value of the excitation flux density distribution can be related to the remanent flux density and the relative permeability of the PMs by the following expression [1]:

$$B_g = \frac{l_m/\mu_r}{l_m/\mu_r \cdot 1/C_\phi + K_c l_g (1 + p_{r1})} \cdot B_r \quad (5)$$

where C_ϕ is the flux focusing factor, K_c is Carter's coefficient and p_{r1} is the normalised rotor leakage permeance. The range of values for p_{r1} is typically 0.05 - 0.2 [1].

B. Synchronous Reactance

The effective airgap in a PM machine with magnets mounted on the rotor surface can be considered constant and relatively large. This is due to the relative permeability of the PM material being close to unity. The d and q -axis synchronous reactances are consequently identical in this machine. The synchronous reactance of the machine can be written in terms of the magnetising (X_m) and leakage (X_l) reactances, as:

$$X_s = X_m + X_l \quad (6)$$

The magnetising reactance can be expressed as [1]:

$$X_m = \frac{6\mu_0 l D f K w_1^2 N_{ph}^2}{p^2 (K_c l_g + l_m/\mu_r)} \quad (7)$$

where the term $K_c l_g + l_m/\mu_r$ in (7) represents the effective airgap length in the path of the magnetising flux. This includes the mechanical airgap clearance modified by Carter's coefficient to account for slotting and the radial thickness of the PMs.

The leakage reactance can be written in terms of the specific permeance coefficients associated with the dominant leakage flux paths of the stator, i.e. the slot, tooth-top and winding overhang leakage flux paths, as [3],[4]:

$$X_l = 4\pi\mu_0 f \frac{N_{ph}^2 l}{pq} (\lambda_{slot} + \lambda_{tooth-top} + \lambda_{overhang}) \quad (8)$$

C. Armature Resistance

The per-phase resistance of the stator winding can be estimated on the basis of the total length of a phase winding. This can be expressed as [2]:

$$l_{ph-winding} = 2(l + l_{end}) \cdot N_{ph} \quad (9)$$

Furthermore, the per-phase resistance of the stator winding, neglecting the skin effect, can be expressed as [2]:

$$R_a = \frac{l_{ph-winding}}{a \cdot \sigma_{cu} \cdot A_{cond}} \quad (10)$$

D. Machine Performance

The efficiency of the PM synchronous machine operated as a generator can be expressed as $\eta = P_L/P_{shaft}$, where P_{shaft} is the input mechanical power applied to the shaft of the machine and P_L is the total real power delivered to its load. The input mechanical and load powers can further be related by:

$$P_{shaft} = P_L + P_{Cu} + P_{rot} + P_{core} \quad (11)$$

where P_{Cu} is the total stator copper losses, P_{rot} is the total rotational losses and P_{core} is the total core losses in the machine.

The total real power delivered to a load on the generator can be expressed as [4]:

$$P_L = 3V_a I_a \cos \phi \quad (12)$$

The total stator copper losses can be expressed as:

$$P_{Cu} = 3I_a^2 R_a \quad (13)$$

The total rotational losses in the machine consist of friction losses in the bearings $P_{friction}$ and windage losses $P_{windage}$. The total rotational losses can therefore be written in terms of its component losses as $P_{rot} = P_{friction} + P_{windage}$.

The total core losses in the machine can be estimated on the basis of the hysteresis loss densities in the stator teeth and yoke (p_{ht} , p_{hy}), and the average eddy current loss densities in the stator teeth and yoke (\bar{p}_{et} , \bar{p}_{ey}). The total core losses can therefore be expressed as [3],[6]:

$$P_{core} = V_{teeth} (p_{ht} + \bar{p}_{et}) + V_{yoke} (p_{hy} + \bar{p}_{ey}) \quad (14)$$

where V_{teeth} and V_{yoke} are the volumes of the stator teeth and yoke, respectively.

IV. EXPERIMENTAL VERIFICATION OF THE ANALYTICAL MODEL

The analytical model of the PM synchronous machine is verified in this section before it can be used to investigate the effect of design changes on the performance of the machine. This is achieved by comparing the calculated equivalent circuit parameters and power losses of a test machine, to the values measured by laboratory experiments.

The design specifications of the test machine used to verify the analytical model are summarised in Table V of the Appendix. The test machine did however have 6 discrete 4x10x50mm NdFeB PMs per pole with a 1mm spacing between PMs, instead of a single smooth PM assumed in the analytical model above. The form factor of the excitation field (4), was thus modified to account for the discrete PMs per pole [2],[5]. The resulting rms value of the fundamental excitation voltage calculated for this machine was compared with that predicted by a Finite Element Analysis (FEA) and the measured voltage at various speeds. This is illustrated in

Fig. 1.

The calculated and measured flux per pole, armature resistance and excitation voltage at 50Hz is shown in Table I.

The variation of calculated and measured core and rotational losses with speed is illustrated in Fig. 2.

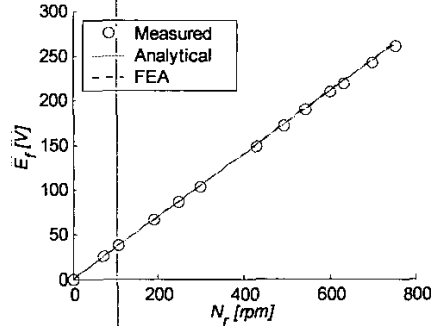


Fig. 1. Comparison of measured and calculated rms value of fundamental excitation voltage at various rotor speeds (N_r)

TABLE I
COMPARISON OF MEASURED AND CALCULATED EQUIVALENT CIRCUIT PARAMETERS FOR THE TEST MACHINE

	Measured	Analytical	FEA
ϕ_p [wb]	0.002264	0.002293	0.002303
E_f [V]	258.77	262.18	263.13
R_a [Ω]	1.317	1.571	-

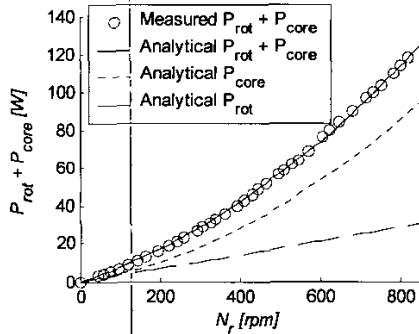


Fig. 2. Variation of core and rotational losses with speed

From the results presented in this section it can be seen that good agreement exists between the calculated and measured equivalent circuit parameters of the test machine, thereby verifying the analytical model of the PM Synchronous machine presented in the previous section.

V. TERMINAL VOLTAGE CHARACTERISTIC AND OPERATING CONDITIONS OF A SMALL PM WIND GENERATOR

In general, small PM wind generators are connected to power electronic converters of varying sophistication. These may vary from simple rectifiers to converters with elaborate control strategies, capable of full four-quadrant operation. In this paper, it is assumed that the generator is connected to a power electronic converter, which operates as an active

rectifier. The armature current of the generator is thus assumed sinusoidal and controlled by the converter. Moreover, the perceived load power factor at the terminals of the machine is also controlled by means of the converter. Under steady-state conditions, the converter can therefore be fully characterised by the generator armature current $I_a \angle \phi$ demanded by a fictitious load Z_L , connected to each phase of the generator. This configuration resembles that of a synchronous machine connected to an isolated load. The steady-state terminal voltage characteristic of an isolated PM synchronous generator is therefore analysed in this section together with its operating power capability.

A. Terminal Voltage Characteristic

The steady-state terminal characteristic of an isolated PM synchronous generator can be determined by considering its per-phase equivalent circuit and phasor diagram. For a synchronous generator with negligible saliency, this can be expressed as:

$$V_a = \sqrt{E_f^2 - (I_a X_s \cos \phi + I_a R_a \sin \phi)^2 + I_a X_s \sin \phi - I_a R_a \cos \phi} \quad (15)$$

Equation (15) can be used to plot a family of curves to illustrate the variation of the generator terminal voltage with equivalent circuit parameters.

B. Operating Conditions

In this section, the terminal voltage characteristic and power capability of the generator are used to explore its steady-state operating conditions. Equation (12) can be used to write an alternate expression for the terminal voltage of an isolated PM synchronous generator. Thus, by solving for V_a , (12) can be rewritten as a function of I_a and P_L , as:

$$V_a = \frac{P_L}{3 \cos \phi} \cdot \frac{1}{I_a} \quad (16)$$

Equation (16) can be used to plot the V_a vs I_a variation required in order for the generator to deliver P_L (kW) to its load, at a specific power factor. The constant per-phase apparent power (VA) hyperbolas obtained in this manner are illustrated in Fig. 3, together with the terminal voltage characteristic of the generator at various operating speeds. The terminal characteristic relates to operation of the generator at a constant load power factor of 0.76 leading, over a range of speeds from 60% to 120% of its rated speed.

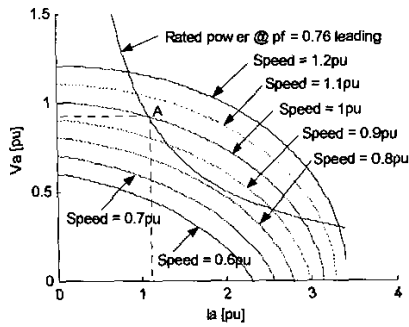


Fig. 3. Constant per-phase apparent power hyperbola with terminal voltage characteristic of generator at various speeds

Point A in Fig. 3, defines the terminal voltage and current at which the machine will operate when required to deliver rated power at rated speed to an isolated load at a power factor of 0.76 leading. Moreover, the intersections between the terminal voltage characteristic curves and the constant per-phase apparent power hyperbola determines the operating points of the generator when required to deliver this power to a load at various speeds.

The operating points can be determined by equating the expressions for each of the curves. This results in a 4th order polynomial, which when solved for the smallest positive real roots results in the armature current that the generator will operate at when delivering the required real power to its load at the specified speeds and power factor.

The operating currents obtained in this manner can be used to evaluate the performance of the generator when delivering the required real power to its load at various speeds. Furthermore, it can be used to evaluate the performance of the generator when design changes are investigated in order to restore the output power capability of the generator at low operating speeds.

VI. EFFECTS OF DESIGN CHANGES ON THE PERFORMANCE OF THE GENERATOR

The output power capability of the generator at low speed operation can be restored through several design improvements. The effects of several changes to the generator design are investigated in this section. The main design changes necessary in order to restore the output power capability of the generator are evaluated on the basis of the overall efficiency of the generator, its equivalent circuit parameters, the mass of active materials used and the flux density levels in the main parts of the generator. The effect of each design change is analysed independently, with all other parameters at nominal values. The nominal design specifications of the machine under consideration are summarised in Table V of the Appendix.

A. Change in the Number of Stator Turns Per Phase (N_{ph})

The first design change investigated in order to restore the output power capability of the generator at low speeds, was an increase in the number of turns per phase. The effect of this

design change on the efficiency of the generator is illustrated in Fig. 4.

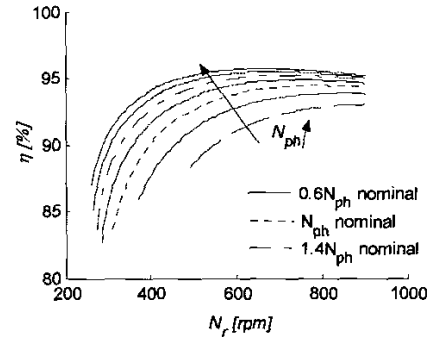


Fig. 4. Effect of a change in the number turns per phase (N_{ph}) on the efficiency of the generator

The family of curves in Fig. 4 illustrates the variation of the generator efficiency with speed, as the number of turns per phase is increased from 60% to 180% of the nominal value, in 20% intervals. Furthermore, the dotted line represents the variation in generator efficiency, when all its design specifications are at nominal values. It can be seen from the figure that the generator becomes capable of delivering rated power to its load at lower speeds as the number of turns per phase is increased. Moreover, the efficiency of the generator improves with an increase in the number of turns per phase when delivering rated power to the load at reduced speeds. The effect of this design change on the efficiency and on two other performance indicators is summarised in Table II. With reference to the table, the specific electric loading (SEL) is the rms value of the stator peripheral current density and J is the stator conductor current density [4].

TABLE II
COMPARISON OF MACHINE PERFORMANCE AT FULL-LOAD, FOR CHANGE IN N_{ph} , AT RATED SPEED (750RPM) AND REDUCED SPEED OPERATION

Speed	Performance	Change in N_{ph}		
		1x	1.2x	1.6x
750 rpm	η [%]	94.44	94.89	95.45
	SEL [A-Cond./m]	19,035	18,977	18,905
	J [A/mm ²]	1.486	1.234	0.922
300 rpm	η [%]	-	85.67	89.61
	SEL [A-Cond./m]	-	48,584	46,174
	J [A/mm ²]	-	3.159	2.252

With reference to Table II, the relatively high efficiency at rated speed is a direct result of the low operating current density due to oversized conductors, and the low armature current required due to the large excitation voltage induced in the stator winding by its many turns per phase. The machine with nominal design specifications is unable to deliver rated power to a load, whilst operating at 300rpm. Increasing N_{ph} makes operation at 300rpm possible, whilst maintaining the relatively high efficiency and low current density. The SEL

does however increase to high values at this low operating speed.

The change in N_{ph} has an effect on the equivalent circuit parameters of the generator. This is illustrated in Fig. 5.

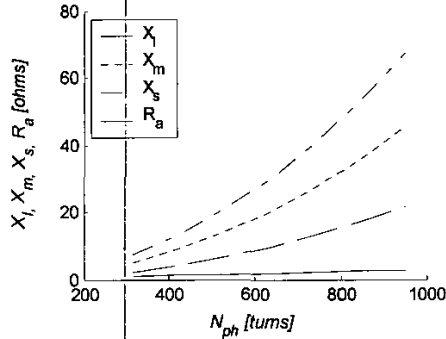


Fig. 5. Effect of a change in the number turns per phase (N_{ph}) on the equivalent circuit parameters at 50Hz

With reference to Fig. 5, it can be seen that the magnetising and leakage reactances increase significantly, as these are proportional to the square of N_{ph} . A 40% increase in N_{ph} will thus result in a 96% increase in the reactances. Furthermore, the armature resistance increases linearly as the total length of copper increases with N_{ph} . The slot-fill factor increases proportionately with this design change. In assessing the machine under consideration, it was observed that the stator slots would only be able to accommodate a 10% increase in the slot-fill factor.

The mass of the copper used in the machine windings increases proportionately with N_{ph} . The copper mass increases by 60%, from 23.63kg to 37.81kg, as N_{ph} is increased from its nominal value (528 turns) by 60%. The mass of the stator core, rotor core and PM material used in the machine remains constant as the number of turns is increased. The power to weight ratio of the machine is therefore not decreased significantly as the number of turns per phase is increased to restore the output power capability of the generator at low speeds.

The flux density levels in the main parts of the machine remain within acceptable limits as N_{ph} is increased. The peak value in the stator teeth and yoke remain constant at 1.80T and 0.504T, whilst the plateau and peak value of the fundamental airgap flux density are 0.756T and 0.851T.

B. Compromised Machine Design for Low Speed Operation

By considering the effects of individual changes to the machine design presented in the previous sections, a compromised design, which combines several changes simultaneously, is investigated in this section. The compromised design would be capable of delivering rated power at low speeds required by a small direct-drive WECS.

An increase in the N_{ph} and A_{cond} results in satisfactory full-load performance at low speeds. However, the copper mass and the slot-fill factor increases proportionately with each of these design changes. Moreover, the actual stator slots can only accommodate a 10% increase in the slot-fill factor. The

reactances of the machine also increase significantly, with the square of the N_{ph} .

The constraint on increasing the axial length of the machine is the reduction in the power to weight ratio of the machine. Similarly, the constraint on increasing α and B_r is the increase in flux density levels in main parts of the machine. In particular, B_{tmax} increases significantly beyond its operating range.

In a compromised design a 40% increase in N_{ph} and a 30% reduction in A_{cond} results in a 10% nett increase in the slot-fill factor and the copper mass. The reduction in A_{cond} is tolerable due to the relatively low operating current density. However, in order to limit the reactances of the machine, N_{ph} was reduced by 30% and A_{cond} increased by 40% instead. A 10% nett increase in the slot-fill factor and the copper mass was therefore still maintained. Furthermore, B_r was only increased by 10% in order to limit B_{tmax} , and α by 30% in the compromised design of the machine. The axial length of the machine was also increased by 40%.

The nominal and compromised design specification of the generator is compared in Table III. The equivalent circuit parameters, flux density levels and total mass is also compared in the table. The efficiency of the generator with nominal and compromised design specifications is compared in Fig. 6. The full-load performance of the generator with compromised design specifications is summarised in Table IV, for operation at various reduced speeds.

TABLE III
COMPARISON OF NOMINAL AND COMPROMISED DESIGN SPECIFICATION OF THE GENERATOR

Parameter	Nominal specification	Compromised specification
N_{ph} [turns]	528	370
l [m]	0.0475	0.0665
α	0.696	0.905
B_r [T]	1.06	1.166
A_{cond} [mm ²]	3.142	4.398
R_a	1.571	0.842
L_l [mH]	21.4	12.165
L_m [mH]	44.6	30.574
L_s [mH]	66.0	42.739
B_g [T]	0.753	0.838
B_{lmax} [T]	0.851	1.054
B_{tmax} [T]	1.804	2.0067
B_{ymax} [T]	0.504	0.729
Total mass [kg]	67.07	85.93
Power/weight [Kw/kg]	521.87	407.29

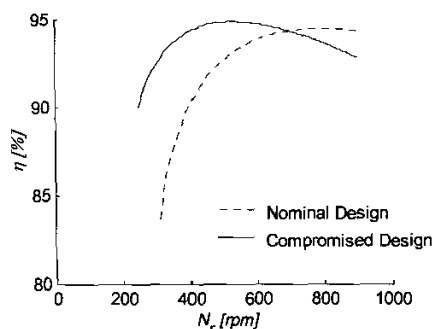


Fig. 6. Comparison of efficiency of the generator with nominal and compromised design specifications

TABLE IV
FULL-LOAD PERFORMANCE OF GENERATOR WITH COMPROMISED DESIGN SPECIFICATIONS, FOR OPERATION AT VARIOUS REDUCED SPEEDS

N_r [rpm]	Full-load performance		
	η [%]	SEL [A-Cond./m]	J [A/mm ²]
255	90.43	32,657	2.600
270	91.21	30,839	2.456
300	92.38	27,812	2.215
330	93.20	25,375	2.021

It can be seen that the generator is capable of full-load operation at low speeds, whilst operating at a good efficiency. The SEL of the generator is also at reasonable values. The operating current density is however low due to the large cross-sectional area of the stator conductors.

VII. CONCLUSIONS

This paper outlined a procedure of adapting a small, standard, readily available PM synchronous machine for direct coupling to a small wind turbine. This was achieved through several minor changes to the nominal design of the machine. The machine with a compromised design was shown to deliver rated power at reduced speeds, suitable for direct-coupling to a small WECS. Moreover, the overall performance of the compromised design was shown to be quite good.

VIII. APPENDIX

The nominal design specifications of the machine under consideration are summarised in Table V below.

TABLE V
NOMINAL DESIGN DATA OF THE PM SYNCHRONOUS MACHINE

Design specification	Value
P - Rated Power	3.5kW
p - Number of pole pairs	4
l - Effective length of stator core	0.0475m
D - Stator inner diameter	0.2472m

l_g - Mechanical airgap clearance	0.0008m
N_{ph} - Number of turns per phase	528
a - Number of parallel paths	1
σ_{Cu} - Conductivity of Cu at 25°C	$57 \cdot 10^6$ S/m
A_{con} - Cross-sectional area of conductors	$\pi \cdot 10^{-6}$ m ²
S - Number of stator slots	36
τ_c - Stator coil pitch	$180 \text{ } \varnothing d$
α - Pole-arc to pole-pitch ratio	0.696
w_t - Width of a stator tooth	0.009m
h_t - Height of stator tooth	0.0387m
h_{11} - Height of conductor portion of slot	0.026m
h_{12} - Height of slot above conductors	0m
h_{13} - Height of tapered portion of slot	0.0026m
h_{14} - Height of stator slot opening	0.0012m
b_{11} - Width of oval portion of stator slot	0.0178m
b_{12} - Width of slot above conductors	0.0132m
b_{13} - Width of tapered portion of slot	0.0132m
b_{14} - Width of stator slot opening	0.0036m
h_s - Height of stator slot	0.0387m
h_y - Height of stator yoke	0.0504m
l_m - Radial thickness of PM	0.004m
B_r - Remanent flux density of PM	1.06T
μ_r - Relative permeability of PM	1.0042
μ_0 - Permeability of free air	$4\pi \cdot 10^{-7}$
ρ_{pm} - Mass density of PM material	7500kg/m ³
ρ_{rc} - Mass density of rotor core material	7860kg/m ³

IX. ACKNOWLEDGMENT

The authors gratefully acknowledge the financial and other support of the University of Cape Town, Eskom and the National Research Foundation (NRF), all of South Africa. The assistance by Mr Chris Wozniak and Mr M. Mathebe in the Electrical Machines Laboratory at the University of Cape Town is also acknowledged.

X. REFERENCES

- [1] T. J. E. Miller, *Brushless Permanent-Magnet and Reluctance Motor Drives*, New York: Oxford University Press, 1989.
- [2] J. F. Gieras, M. Wing, *Permanent Magnet Motor Technology: Design and Applications*, 1st ed., New York: Marcel Dekker, 1997.
- [3] G. R. Slemon, "Design of Permanent Magnet AC Motors for Variable Speed Drives," in *Tutorial Course IEEE-IAS Annual Meeting*, P. Pillay, Ed. Michigan: IEEE, 1991, pp. 3-1 - 3-35.
- [4] M. G. Say, *The Performance and Design of Alternating Current Machines*, 3rd ed., London: Pitman & Sons, 1965.
- [5] M. Wing, "Analysis of an Energy Efficient Permanent Magnet Brushless Universal Motor," Ph.D. dissertation, Dept. Elec. Eng., Univ. Cape Town, South Africa, 1996.
- [6] G. R. Slemon, and X. Liu, "Core Losses in Permanent Magnet Motors," *IEEE Trans. Magnetics*, vol. 26, pp. 1653-1655, Sep. 1990.

XI. BIOGRAPHIES

Azeem Khan (S'02) received the B.Sc. and M.Sc. degrees in Electrical Engineering from the University of Cape Town, South Africa in 1994 and 2001, respectively. He is currently working toward a Ph.D. in electrical engineering at the University of Cape Town. His field of interest is electric machines and drives.

Dr Pragasen Pillay (S'84, M'87, SM'92) received the Bachelor's degree from the University of Durban-Westville in South Africa in 1981, the Master's degree from the University of Natal in South Africa in 1983 and the Ph.D from the Virginia Polytechnic Institute & State University in 1987, while funded by a Fulbright Scholarship. From January 1988 to August 1990 he was with the University of Newcastle upon Tyne in England. From August 1990 to August 1995 he was with the University of New Orleans. Currently he is with Clarkson University, Potsdam, NY 13699, where he is a Professor in the Department of Electrical & Computer Engineering and holds the Jean Newell Distinguished Professorship in Engineering. He is a Senior Member of the IEEE and a member of the Power Engineering, Industry Applications, Industrial Electronics and Power Electronics Societies. He is a member of the Electric Machines Committee, Past-Chairman of the Industrial Drives within the Industry Applications Society and Chairman of Induction Machinery Sub-Committee in the Power Engineering Society. He is a member of the IEE, England and a Chartered Electrical Engineer. He has organized and taught short courses in electric drives at the Annual Meeting of the Industry Applications Society. His research and teaching interests are in modeling, design and control of electric motors and drives for industrial and alternate energy applications.

Michel Malengret received the B.Sc. degree in electrical engineering from the University of Natal, South Africa in 1976 and the M.Sc. degree in electrical engineering from the University of Cape Town, South Africa in 1978. He has extensive experience in Power Electronics and is currently the director of his own company, which specialises in the development of inverter and UPS systems. He is also currently working toward a Ph.D. in electrical engineering at the University of Cape Town, where he holds a position as Senior Lecturer in the Department of Electrical engineering. His fields of interest are electric machines and drives, Power Electronics, Renewable Energy Systems and Power Distribution.